Research Square

Preprints are preliminary reports that have not undergone peer review.
They should not be considered conclusive, used to inform clinical practice,
or referenced by the media as validated information.

The influence of the coincidence coefficient between the grinding direction and the dressing direction on the grinding quality

Junming Wang

w.jm@hbut.edu.cn

Hubei University of Technology https://orcid.org/0009-0000-6855-6433

Wei Chen

Hubei University of Technology

Jing Li

Hubei University of Technology

Research Article

Keywords: CBN grinding wheel, Anastomosis coefficient, Diamond roller, Diamond pen

Posted Date: November 18th, 2026

DOI: https://doi.org/10.21203/rs.3.rs-11621740/v1

License: This work is licensed under a Creative Commons Attribution 4.0 International License.
Read Full License

The influence of the coincidence coefficient between the grinding direction and the dressing direction on the grinding quality

Junming Wang* · Wei Chen · Jing Li
College of Mechanical Engineering, Hubei University of Technology, Wuhan, 430068, China
*Corresponding author: Junming Wang, E-mail: wjm@hbut.edu.cn

Abstract

In grinding wheel dressing technology, it is important to improve the grinding force of the grinding wheel. In this paper, the dressing technology of current CBN grinding wheels is studied, and the hypothesis of the influence of grinding direction and dressing direction on grinding is proposed: "Under the same conditions, when the dressing direction of the grinding wheel is the same as the grinding direction, the grinding capacity of the grinding wheel is the strongest, i.e., the required grinding force is the smallest and the grinding wheel wear is the smallest." This hypothesis is verified by establishing the coefficient of overlap between the grinding direction and the dressing direction and by building the related mathematical model. It provides a new idea for the traditional surface grinding method: the moving direction of the table will change with the dressing direction and is no longer perpendicular to the spindle direction of the grinding wheel. Finally, based on the spatial grid theory, a theoretical model of the grinding surface is established, and the influence of the coincidence coefficient on the grinding surface is analyzed to guide surface grinding and to improve the grinding capacity of the grinding wheel.

Keywords *CBN grinding wheel · Anastomosis coefficient · Diamond roller · Diamond pen*

1 Introduction

With the continuous development of grinding technology, grinding tools have been further improved. At present, there are two main types of grinding wheels on the market: one is aluminum oxide grinding wheels, and the other is ceramic bonded cubic boron nitride (CBN) superhard grinding wheels. The former can cause serious adhesion and wear problems when machining certain hard materials, such as nickel-based high-temperature alloys [1]. The latter has good thermal stability when machining hard materials, strong chemical inertia, good wear resistance, and low overall machining costs [2].

CBN grinding wheel is composed of cubic boron nitride abrasive and binder. In the grinding process, due to the grinding force, high temperature, and adhesion in the grinding area, the grinding grains on the working surface of the grinding wheel will gradually blunt and lose the cutting edge. At the same time, the wheel surface will lose the correct geometry due to the uneven wear and shedding of abrasive particles. In addition, it is easy to block the gap of the working surface of the grinding wheel due to the very small debris in high-speed grinding. In order to give full play to the performance of superhard abrasive grinding wheel, and to always keep the grinding wheel in a good state of grinding and surface topography, the grinding wheel must be dressed after a period of grinding, in order to obtain better processing efficiency, dimensional accuracy, and surface precision. Otherwise, it will lead to an increase of grinding force, deterioration of grinding conditions, and an increase of temperature in the grinding zone, which affects the surface integrity of the workpiece and shortens the grinding wheel life. Therefore, it is of great significance to research and develop dressing technology of high-efficiency and high-precision superabrasive grinding wheels.

In order to study the dressing problems of CBN grinding wheels, researchers have put forward many new dressing methods, such as laser dressing technology [3], ELID, electrolytic in-process dressing [4], electric discharging dressing, ultrasonic vibration dressing [5], ultrasonic roller dressing [6], etc. Although there are new dressing methods, mechanical dressing is still the mainstream in the market, and mechanical dressing can keep CBN grinding wheel in a good state. Diamond tools have good chemical and physical properties, and the dressing methods used in production are still the rotary diamond roller dressing method and the diamond pen dressing method [7].

In terms of wheel dressing, Uchida et al. [8] judged the situation of wheel dressing by quantitatively analyzing the surface state of the grinding wheel. Li et al. [9] designed and carried out the grinding experiment of a single diamond abrasive dresser on the V-CBN abrasive segment, and found that different trajectory lengths lead to different wear forms of diamond abrasives and vitrified bond of V-CBN grinding wheels. In 2019, Shi et al. [10] explored the influence of different contents of nanomaterials on the performance of grinding wheels. Through grinding experiments, it was proved that the grinding force and grinding temperature of nano vitrified bond grinding wheels were lower than those of conventional vitrified bond grinding wheels, and the grinding surface quality was better than that of conventional vitrified bond abrasives. Nano vitrified bond CBN grinding wheels are more suitable for grinding of superalloys. In 2021, Wang et al. [11] simplified the honing wheel dressing process into a grinding wheel dressing process, and studied the progressive fracture evolution, stress characteristics, and fracture mode of CBN abrasive grains during the dressing process. It was found that the fracture evolution of CBN grains mainly experienced four stages: elastic deformation, damage initiation, crack formation, and macroscopic fracture. Macerol et al. [12]

proposed a new method based on grinding to study the wear behavior of the abrasive-bonding system. The wear test was carried out in grinding, surface grinding, and cylindrical grinding. A series of abrasive shape aspect ratios and abrasive toughness values of the same abrasive-bonding system can be used, which greatly saves the dressing time.

In terms of grinding force of grinding wheels, in 2019, Shi et al. [10] demonstrated through high grinding experiments that the grinding force and grinding temperature of nano ceramic bond grinding wheels were lower than those of conventional ceramic bond grinding wheels, and the grinding surface quality was better than that of conventional ceramic bond abrasives. Dai et al. [13] conducted grinding experiments to investigate the effect of undeformed chip thickness nonuniformity and found that the specific grinding force increased with increasing mean value, decreasing standard deviation, and increasing percentage of active grits, and the specific grinding energy increased with decreasing mean value, increasing standard deviation, and increasing percentage of active grits; the undeformed chip thickness nonuniformity had an effect on the specific grinding force and specific grinding energy. Xiao et al. [14] developed metal-bonded cubic boron nitride (CBN) grinding wheels using an open hole structure and found that the grinding force and grinding temperature of sintered porous agglomerated state CBN grinding wheels decreased and maintained a stable grinding force ratio of 2.5.

Lin et al. [15] found that the speed and feed of the abrasive had a significant effect on the surface roughness and tooth wear. Chen et al. [16] believe that dressing plays a decisive role in grinding performance, affecting the grinding surface, material removal rate, and cooling conditions of the tool. Ding et al. [17] showed that with the continuous wear of abrasives and abrasives, the influence of brazing induced stress was significant. Fang et al. [18], after analyzing grinding wheel appearance, diameter, grinding force, and workpiece surface roughness, concluded that

workpiece surface roughness is the best evaluation index of the grinding wheel wear process. In the grinding of triangular abrasive wheel, Curtis et al. [19] found that different dressing mechanisms had a leading effect on the dressing morphology. Shi et al. [20] improved the working performance of the dressing wheel by modifying its parameters. Uchida et al. [21] proposed a recalculation method for measuring the focus position and proved that the multi-screw dressing method can improve the dressing efficiency of grinding tools by measuring the grinding wheel surface after grinding. Kannan et al. [22] established a prediction model of abrasive tools, used a Hall effect sensor to measure motor current, and communicated the information with the operator's Android device, so that the abrasive tools could be repaired automatically when they reached the limit of use. Godino et al. [23] analyzed the dressing parameters of fixed multi-point dressing tools and blade dressing tools, and came to the conclusion that dressing tools and dressing parameters were particularly important to the dressing of grinding tools. Li et al. [9] came to the conclusion, through grinding experiments in the study of the correction process of CBN grinding wheel, that the influence of the corrected feed on the grinding force was greater than that of the corrected depth.

In the previous studies, dressing parameters are separated from grinding parameters. This paper will try to find out the internal relationship between dressing parameters and grinding parameters. The purpose is: when given grinding parameters, the range of optimal dressing parameters can be reduced; or find the best grinding parameter range corresponding to a certain dressing parameter. Thus, it can avoid aimlessly dressing the wheel, reduce dressing cost, and improve dressing efficiency.

2 Theoretical exploration

According to the hypothesis: dressing parameters and grinding parameters can be connected by the degree of coincidence between the dressing direction and the grinding direction. Under the same conditions, when the dressing direction of the grinding wheel is consistent with the grinding direction, the grinding ability of the grinding wheel is the strongest, that is, the grinding force required is the least, and the grinding wheel wear is the least. In this paper, when studying the dressing technology of CBN grinding wheel, the matching coefficient of grinding direction and dressing direction is introduced to establish the relevant mathematical model. The specific theoretical exploration is as follows.

The dressing experiment and surface grinding experiment of CBN grinding wheel were carried out with a single point diamond pen. Mathematical models of grinding force, surface roughness, and grinding wheel wear based on material removal amount were established. The effects of different grinding directions and dressing directions on various grinding parameters in surface grinding were analyzed and compared.

In order to analyze the variation relationship of each parameter when the dressing direction is different from the grinding direction, we used it as the coincidence coefficient of the grinding direction and the dressing direction, and let:

$$\xi = 1 - I\varphi - \beta I / \varphi \tag{1}$$

In Eq. (1), φ is the trimming angle, and β is the grinding angle.

According to the theoretical knowledge of space engagement, the surface model of the dressed grinding wheel was first established, and then the surface mathematical theoretical models of external grinding and surface grinding were established respectively, and the influence of the coincidence coefficient on the residual height and surface texture was analyzed.

When dressing grinding wheel with single point diamond pen, the speed diagram of the contact point and the dressing direction are shown in Fig. 1.

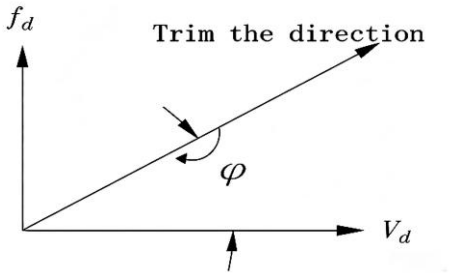


Fig. 1 The speed diagram of the contact point and the dressing direction

In Fig. 1, v_d is the grinding wheel linear speed during dressing, f_d is the axial moving speed, and φ is defined as the dressing direction angle, then

$$\varphi = acrtanf_d / v_d \tag{2}$$

In the traditional plane grinding process, the moving direction of the workpiece is perpendicular to the axis of the grinding wheel, and the velocity of the contact point between the abrasive particle and the workpiece can be expressed as the grinding direction being consistent with the moving direction of the workbench. If we deviate the movement direction of the table by a certain angle, as shown in Fig. 2, the grinding direction is indicated by β. The relation between β and α can be obtained by using the parallelogram rule as follows:

$$v_w sin(\alpha - \beta) = v_s sin\beta \tag{3}$$

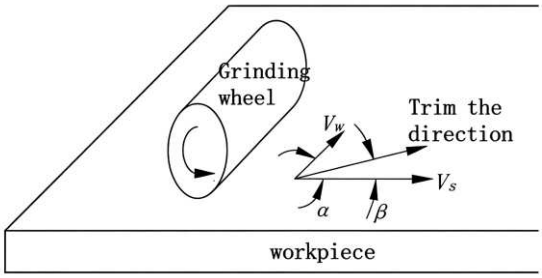


Fig. 2 Schematic diagram of plane grinding

When the grinding direction is consistent with the dressing direction, there is $\beta = \varphi = arctanf_d / v_d$ substitute into Eq. (3), you can obtain the moving speed direction of the table α.

For CBN grinding wheels with different particle sizes, the traditional grinding method and the dressing direction are consistent with the grinding direction. According to the experimental data and the least square method, the dynamic prediction model of each parameter based on dressing direction and workpiece grinding amount was constructed, and the changes of each parameter were tracked in real time. The differences of each model under the traditional grinding method and the same dressing direction and grinding direction were analyzed and compared, and the actual production was guided.

$$\begin{cases} F\mathrm{n} = f_{F\mathrm{n}}\left(V_\mathrm{s},\ V_\mathrm{w},\ \alpha_\mathrm{p},\ Q,\ \alpha_\mathrm{d},\ f_\mathrm{d},\ \phi\right) \\ F\mathrm{t} = f_{F\mathrm{t}}\left(V_\mathrm{s},\ V_\mathrm{w},\ \alpha_\mathrm{p},\ Q,\ \alpha_\mathrm{d},\ f_\mathrm{d},\ \phi\right) \\ F\alpha = f_{F\alpha}\left(V_\mathrm{s},\ V_\mathrm{w},\ \alpha_\mathrm{p},\ Q,\ \alpha_\mathrm{d},\ f_\mathrm{d},\ \phi\right) \\ R\alpha = f_{R\alpha}\left(V_\mathrm{s},\ V_\mathrm{w},\ \alpha_\mathrm{p},\ Q,\ \alpha_\mathrm{d},\ f_\mathrm{d},\ \phi\right) \\ \Delta\mathrm{r}/\mathrm{r}_0 = f_{\Delta\mathrm{r}/\mathrm{r}_0}\left(V_\mathrm{s},\ V_\mathrm{w},\ \alpha_\mathrm{p},\ Q,\ \alpha_\mathrm{d},\ f_\mathrm{d},\ \phi\right) \end{cases} \quad (4)$$

In Eq. (4), the meaning of parameters in the model: $F\alpha$ is the axial grinding force; Fn is the normal grinding force; Ft is the tangential grinding force; $R\alpha$ is the surface roughness; $\Delta r/r_0$ is the grinding wheel removal rate; V_s is the grinding wheel speed; V_w is the workpiece feeding speed; α_p is the grinding depth; Q is the workpiece grinding amount; f_d is the dressing feed speed; α_d is the dressing feed; ϕ is the direction of decorating.

3 The surface mathematical model of surface grinding and external grinding is established

Fig. 3 shows the schematic diagram of diamond pen dressing cylindrical grinding wheel. In Fig. 3, the unit vectors of the three coordinate axes are i, j, and k. Set the diameter of the cylindrical grinding wheel as d_s, the dressing depth as a_d, the grinding speed as n_0, and the feed speed as f_d. In order to simplify the calculation, the diamond pen is simplified into a triangular cutting edge as shown in Fig. 4, and the angle of the cutting edge is θ_1.

Assume that the cutting edge actually involved in grinding is the ABC region and the cutting edge coordinate is δ. Therefore, when point A participates in dressing, the dressing depth here is a_d, the initial cutting coordinate of point A is set as (d_s/2, 0, 0), and the cutting time is set accordingly.

According to the meshing principle of spatial helical surfaces, the surface formed at this time is the right helical surface of equal rise cylinder, and the equation of the right helical surface can be expressed as:

$$r = r_0(\delta)(k,\theta)R + p\theta k \tag{5}$$

In Eq. (5), $r_0(\delta) = (d_s/2 - \alpha_d + |\delta|\ Cot\ \theta_1/2)j + \delta k$ are the coordinate vectors of a cutting edge, and $p = f_d/2\pi n_0$ is the spiral parameter.

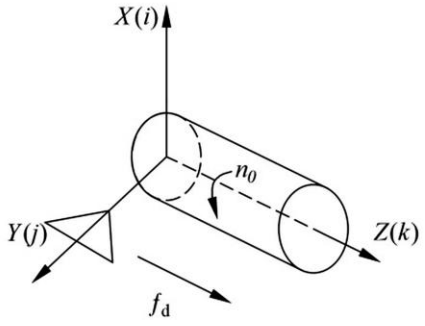


Fig. 3 Schematic diagram of diamond pen dressing cylindrical grinding wheel

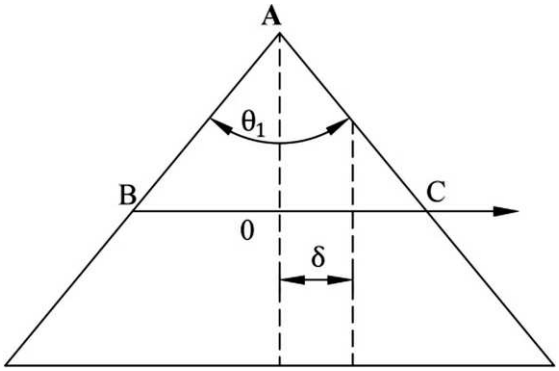


Fig. 4 Section of diamond pen

The angle at which the bus is rotated around the z axis from the beginning is $\theta = 2\pi n0t$, so the vector *r* is expanded and the equation of the right helical surface can be calculated as shown in Eq. (6).

$$\begin{cases} \chi = \left(d_s / 2 - \alpha_d + |\delta| cot\theta_1 / 2\right) sin2\pi n_0 t \\ y = \left(d_s / 2 - \alpha_d + |\delta| cot\theta_1 / 2\right) cos2\pi n_0 t \\ z = f_d t + \delta \end{cases} \tag{6}$$

In Eq. (6), $\delta \in [-\alpha_d tan(\theta_1/2), \alpha_d tan(\theta_1/2)]$, and the helix lead is $p_z = f_d / n_0$.

When $\alpha_d tan(\theta_1/2) \leq p_z/2$, there is no interference when the cutting edge of the diamond pen continues dressing the cylindrical grinding wheel, and the diamond pen is only used for trimming.

When $\alpha_d tan(\theta_1/2) \geq p_z/2$, interference occurs when the cutting edge of the diamond pen continues dressing the cylindrical grinding wheel, and the width of interference $B_1 = \alpha_d tan(\theta_1/2) - p_z/2$. At this time, the diamond pen is both shaped and sharpened. In this case, $\delta \in [-\alpha_d tan(\theta_1/2) + B_1, \alpha_d tan(\theta_1/2) - B_1]$.

After dressing, it is assumed that the abrasive grains are evenly distributed along the spiral line and the cutting edges of the abrasive grains are arranged in the same direction as the dressing. In

order to simplify the mathematical model of grinding surface, the abrasive particles evenly distributed along the spiral line were regarded as continuous spiral cutting edges, and the normal truncation of the cutting edges was triangular. Because the contact area between the grinding wheel and the workpiece is small, this simplified method is feasible when only surface roughness is analyzed. Fig. 5 shows the schematic diagram of establishing the plane grinding coordinate system.

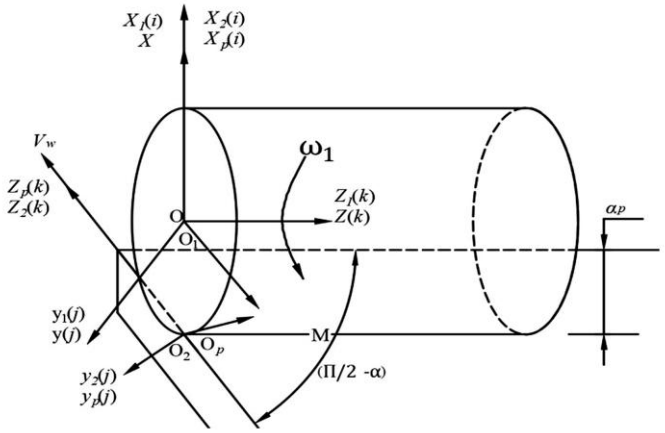


Fig. 5 Schematic diagram of plane grinding coordinate system

In Fig. 5, $s(o\text{-}x, y, z)$ and $s_p(o_p\text{-}x_p, y_p, z_p)$ are two coordinate systems fixed in space. The axis coincides with the rotation axis of the grinding wheel, and z_p points to the moving direction of the workpiece.

The origin of $s_p(o_p\text{-}x_p, y_p, z_p)$ is at the cutting point when the grinding wheel cuts into the workpiece and contacts the workpiece. The angle between the z axis and the z_p axis is $(\pi/2 - \alpha)$. The axis recombines with the x_p axis, $o_p o = d_s/2$.

The coordinate system $s_1(o_1\text{-}x_1, y_1, z_1)$ is fixated with the grinding wheel, and the coordinate system $s_2(o_2\text{-}x_2, y_2, z_2)$ is fixated with the workpiece. At the initial position, they coincide with s and s_p respectively. When working, the grinding wheel rotates around the z axis at a uniform angular speed ω_1. The workpiece moves uniformly along the z_p axis with velocity v_w. After a

period of time from the starting position, the workpiece moves $o_p o_2 = I_2$, and the grinding wheel rotates an angle φ_1 around the z axis.

According to the matrix and coordinate transformation method and Eq. (6), the equation of the cutting edge surface in s_1 can be obtained:

$$\begin{cases} \chi_1 = \left(\mathrm{d}_0/2 - \alpha_\mathrm{d} + |\delta|\sin(\theta_1/2)\right)\cos(2\pi \mathrm{n}_0 \mathrm{t} + \varphi_1) \\ \mathrm{y}_1 = \left(\mathrm{d}_0/2 - \alpha_\mathrm{d} + |\delta|\cot(\theta_1/2)\right)\cos(2\pi \mathrm{n}_0 \mathrm{t} + \varphi_1) \\ \mathrm{z}_1 = f_\mathrm{d}\mathrm{t} + \delta \end{cases} \tag{7}$$

Then the normal vector of any point on the cutting edge surface is:

$$\begin{cases} \mathrm{n}_{\chi_1}^{(1)} = \left(\mathrm{d}_\mathrm{s}/2 - \alpha_\mathrm{d} + |\delta|\cot(\theta_1/2)\right)2\pi \mathrm{n}_0 \sin(2\pi \mathrm{n}_0 \mathrm{t} + \varphi_1) \\ + f_\mathrm{d}\cot(\theta_1/2)\cos(2\pi \mathrm{n}_0 \mathrm{t} + \varphi_1) \\ \mathrm{n}_{\mathrm{y}_1}^{(1)} = \left(\mathrm{d}_\mathrm{s}/2 - \alpha_\mathrm{d} + |\delta|\cot(\theta_1/2)\right)2\pi \mathrm{n}_0 \cos(2\pi \mathrm{n}_0 \mathrm{t} + \varphi_1) \\ + f_\mathrm{d}\cot(\theta_1/2)\sin(2\pi \mathrm{n}_0 \mathrm{t} + \varphi_1) \\ \mathrm{n}_{\mathrm{z}_1}^{(1)} = -\left(\mathrm{d}_\mathrm{s}/2 - \alpha_\mathrm{d} + |\delta|\cot(\theta_1/2)\right)2\pi \mathrm{n}_0 \cot(\theta_1/2) \end{cases} \tag{8}$$

There is a point M on the surface of the cutting edge of the grinding wheel (see Fig. 5), and its coordinate value in the coordinate system s is (x, y, z). According to the grinding schematic diagram, the relative movement speed of the workpiece and the grinding wheel at point M is:

$$\begin{aligned} v^{(12)} &= v^{(1)} - v^{(2)} = -\omega_1 y i + [-w_1 x - V_w \sin(\pi/2 + \alpha)]j \\ &- V_w \cos(\pi/2 + \alpha)k \end{aligned} \tag{9}$$

Parameters of coordinate system s_1 can be expressed as:

$$
\begin{aligned}
v^{(12)} &= [-\omega_1(x_1 sin\ \varphi_1 + y_1 cos\ \varphi_1)]i + \\
&[\omega_1(x_1 cos\varphi_1 - y_1 sin\ \varphi_1) - V_w sin(\pi/2+\alpha)]j \\
&+[-V_w cos(\pi/2+\alpha)]k
\end{aligned} \tag{10}
$$

For two moving objects engaged in space, their relative motion velocity at the contact point is perpendicular to the normal vector, and they meet the meshing equation $v^{(12)} \cdot n = 0$ at the contact point, i.e.

$$
\begin{aligned}
&[-\omega_1(x_1 sin\ \varphi_1 + y_1 cos\varphi_1)]nx_i^{(1)} \\
&+[\omega_1(x_1 cos\ \varphi_1 - y_1 sin\varphi_1) - Vwsin(\pi/2+\alpha)]ny_i^{(1)} + \\
&[V_w cos(\pi/2+\alpha)]n_{zi}^{(1)} = 0
\end{aligned} \tag{11}
$$

In the above formula, ω_1, v_w, and α are respectively the rotation speed of the grinding wheel, the moving speed of the workpiece, and the direction angle of the workpiece moving speed during grinding.

When the grinding direction is inconsistent with the dressing direction, the grinding force increases in the grinding process, the grinding process may contact the workpiece, and the dressing efficiency is low.

When the direction of grinding and dressing is in the same direction, with $v_w\ sin(\alpha - \beta) = v_s\ sin\ \beta = \omega_1 d_s\ sin\ \beta/2$, namely:

$$
v_w = \omega_1 d_s sin\beta / 2sin(\alpha - \beta) \tag{12}
$$

In the above formula, β is the dressing direction angle, and d_s is the grinding wheel diameter. Substitute Eq. (12) into Eq. (11) and cancel ω_1, then:

$$
\begin{aligned}
&[-(x_1 sin\varphi_1 + y_1 cos\varphi_1)]n_{x_i}^{(1)} \\
&+[(x_1 cos\varphi_1 - y_1 sin\varphi_1) - d_s sin\beta sin(\pi/2+\alpha)/2sin(\alpha-\beta)]n_{y_i}^{(1)} \\
&+[d_s sin\beta cos(\pi/2+\alpha)/2sin(\alpha-\beta)]n_{z_i}^{(1)} = 0
\end{aligned}
\quad (13)
$$

In Eq. (13), $n_{x_1}^{(1)}$, $n_{y_1}^{(1)}$, and $n_{z_1}^{(1)}$ are the coordinate values (x_1, y_1, z_1) of a cutting edge point on the surface (that is, the delta parameter δ, t), so this equation is actually the relation of angle φ_1 with (δ, t), which can be expressed as $\varphi_1 = \varphi_1(\delta, t)$.

When the angle φ_1 is constant, a series of points on the cutting edge surface satisfy (δ, t), that is to say, the grinding wheel cutting edge surface is in linear contact with the workpiece.

In the traditional surface grinding method, ω_1 and v_w are independent of each other. There is no functional relationship between them. To satisfy the above meshing equation, the following two independent conditions must be satisfied simultaneously:

$$
\begin{cases}
([-\omega_1(x_1 sin\ \varphi_1 + y_1 cos\ \varphi_1)]n_{x_i}^{(1)} + \\
\omega_1(x_1 cos\varphi_1 - y_1 sin\ \varphi_1)n_{y_i}^{(1)} = 0 \\
\quad -v_w sin(\pi/2+\alpha)n_{y_i}^{(1)} + \\
\quad [v_w cos(\pi/2+\alpha)]n_{z_i}^{(1)} = 0
\end{cases}
\quad (14)
$$

At this point, when the angle φ_1 is constant, only a point (δ, t) on the cutting edge surface can satisfy the relation, that is to say, in the traditional plane grinding method, in the simplified mathematical model, the cutting edge surface of the grinding wheel is in point contact with the workpiece.

The coordinate transformation matrix between coordinate system s_1 and coordinate system s_2 is:

$$M_{21}=\begin{pmatrix} cos\ \varphi_1 & -sin\ \varphi_1 & sin\varphi_1 sin\left(\pi/2+\alpha\right)d_s/2 \\ sin\ \varphi_1 sin(\pi/2+\alpha) & cos\varphi_1 cos(\pi/2+\alpha) & sin\left(\pi/2+\alpha\right) \quad 0 \\ sin\ \varphi_1 sin(\pi/2+\alpha) & sin(\pi/2+\alpha) & cos\left(\pi/2+\alpha\right) \quad -l_2 \\ 0 & 0 & 0 \quad 1 \end{pmatrix} \quad (15)$$

In the formula above, I_2 is the distance that coordinate system s_2 moves, φ_1 is the angle that coordinate system s_1 rotates, $(\pi/2+\alpha)$ is the angle between the axes of z and z_p, and d_s is the diameter of the grinding wheel. That is:

$$(x_2 \quad y_2 \quad z_2 \quad 1)^T = M_{21}(x_1 \quad y_1 \quad z_1 \quad 1)^T \quad (16)$$

According to Eqs. (7)-(8) and (13), and (15)-(16), the position of the contact line can be transformed into s_2, the coordinate system fixedly connected with the workpiece, and (δ, t) can be regarded as a variable to obtain the mathematical model of the grinding surface of the workpiece.

According to Eqs. (7)-(8) and (14), and (15)-(16), the position of the contact point can be transformed into s_2, the coordinate system fixedly connected with the workpiece, and (δ, t) can be regarded as a variable, so the grinding surface mathematical model of the workpiece in the traditional plane grinding method can be obtained.

According to the established mathematical model of grinding surface, the meshing boundary point and interference analysis were carried out to obtain the properties of the mathematical model, and the differences of grinding surface roughness and surface texture under the two grinding modes were analyzed.

3 Conclusion

After theoretical simulation, due to experimental conditions, the hypothesis that "under the same conditions, the dressing direction of the grinding wheel is consistent with the grinding direction, the grinding ability of the grinding wheel is the strongest, that is, the grinding force required is the smallest, and the grinding wheel wear is the smallest" is only theoretically verified, and a mathematical model is established.

The theoretical hypothesis is verified, which can provide a new idea for the traditional plane grinding method: the moving direction of the table will change with the dressing direction, and is no longer perpendicular to the grinding wheel spindle direction. At the same time, dressing parameters and grinding parameters are used together to affect the dressing and grinding of the grinding wheel, avoid aimless dressing of the grinding wheel, reduce dressing cost, and improve dressing efficiency.

Declarations

Funding The authors declare that no funds, grants, or other support were received.

Competing interests The authors have no competing interests to declare that are relevant to the content of this article.

Generative AI and AI-assisted technologies in the writing process During the preparation of this work the authors did not use AI for any aspects. The authors reviewed and edited the content as needed and take full responsibility for the content of the published article.

Author Contributions All authors contributed to the study conception and design. Material preparation, data collection and analysis were performed by Junming Wang, Wei Chen and Jing Li. The first draft of the manuscript was written by Junming Wang and all authors commented on previous versions of the manuscript. All authors read and approved the final manuscript.

References

1. Zhang J (2025) Study on the mechanism of ultrasonic elliptical vibration-assisted drilling of SiCp/Al composites. Doctoral dissertation, Taiyuan University of Science and Technology. https://doi.org/10.27721/d.cnki.gyzjc.2025.000566

2. Mao C, Zhang M, Zhang J et al (2015) The effect of processing parameters on the performance of spark plasma sintered cBN-WC-Co composites. J Mater Eng Perform 24(12):4612–4619

3. Ma R, Ma F, Liu Y et al (2026) Research on digital design and grinding key technologies of superabrasive grinding wheels. Superhard Mater Eng 37(5):1–9

4. Raffles MH, Stephenson DJ, Shore P et al (2011) Electrolytic in-process dressing superfinishing of spherical bearings using metal-resin bond ultra-fine CBN wheels. Proc Inst Mech Eng B J Eng Manuf 225(1)

5. Yang Z, Sun W, He D et al (2021) Effect of laser-assisted ultrasonic vibration dressing parameters of a cubic boron nitride grinding wheel on grinding force, surface quality, and particle morphology. Rev Adv Mater Sci 60(1)

6. Dai J, Li Y, Xiang D (2022) The mechanism investigation of ultrasonic roller dressing vitrified bonded CBN grinding wheel. Ceram Int 48(17):24421–24430

7. Cui ZM, Liu NF (2006) Technique and application about diamond dressing roller. Key Eng Mater 304–305:52–56

8. Uchida G, Yamada T, Iwasaki Y (2023) Evaluation of dressing condition based on quantification of grinding wheel surface conditions. Int J Autom Technol 17(1)

9. Li M, Ding W, Zhao Z et al (2020) An investigation on the dressing contact behavior between vitrified bonded CBN abrasive wheel and diamond grit dresser. J Manuf Process 58:355–367

10. Shi Y, Wang Z, Xu S et al (2019) Study on the grindability of nano-vitrified bond CBN grinding wheel for nickel-based alloy. Int J Adv Manuf Technol 100(5):1913–1921

11. Wang F, Chen Y, Gao Y et al (2021) Peridynamic simulation to fracture mechanism of CBN grain in the honing wheel dressing process. Micromachines 12(10)

12. Macerol N, Franca L, Attia H et al (2022) A lapping-based test method to investigate wear behaviour of bonded-abrasive tools. CIRP Ann Manuf Technol 71(1):305–308

13. Dai C, Yin Z, Ding W et al (2019) Grinding force and energy modeling of textured monolayer CBN wheels considering undeformed chip thickness nonuniformity. Int J Mech Sci 157–158

14. Xiao G, Zhao B, Ding W et al (2021) On the grinding performance of metal-bonded aggregated cBN grinding wheels based on open-pore structures. Ceram Int 47(14):19709–19715

15. Lin HM, Liao YS, Wei CC (2015) Wear behavior in turning high hardness alloy steel by CBN tool. J Manuf Sci Prod 15(7–8):679–684

16. Chen ZZ, Xu JH, Ding WF et al (2015) Grinding temperature during high-efficiency grinding Inconel 718 using porous CBN wheel with multilayer defined grain distribution. Int J Adv Manuf Technol 77(1–4):165–172

17. Ding WF, Zhu YJ, Xu JH et al (2015) Finite element investigation on the evolution of wear and stresses in brazed CBN grits during grinding. Int J Adv Manuf Technol 81:985–993

18. Fang Q, Tong CZ, Tong LQ et al (2018) A study on the evaluation indexes of wear process of electroplated CBN grinding wheel. Mater Sci Forum 940:72–76

19. Curtis D, Novovic D, Ghadbeigi H (2018) The influence of abrasive grit morphology on wheel topography and grinding performance. Procedia CIRP

20. Shi X, Zhou Y, Zhang W et al (2019) A new worm grinding method of face gears based on the optimization of dressing wheel profile. Forsch Ingenieurwes 83(3):751–757

21. Uchida G, Yamada T, Ichihara K et al (2021) Evaluation of grinding wheel surface shape on difference multiple helical dressing condition. Int J Autom Technol 15(1):57–64

22. Kannan K, Arunachalam N, Chawla A et al (2018) Multi-sensor data analytics for grinding wheel redress life estimation: an approach towards Industry 4.0. Procedia Manuf 26:1230–1241

23. Godino L, Pombo I, Sanchez JA et al (2017) Analysis of the dressing process using stationary dressing tools. Procedia Manuf 13:146–152